

Geo-disaster Prediction and Geo-hazard Mapping in Urban and Surrounding Areas Progress Report in FY 2004

Masahiro CHIGIRA, Susumu IAI, Roy C. SIDLE, Toshitaka KAMAI,
Mamoru MIMURA, Hiroshi SUWA, Takashi SAITO,
and Tetsuo TOBITA

Synopsis

Urban development rapidly expanding from lowlands to surrounding hills and mountains poses increasing risks for geo-hazards, including liquefaction during earthquakes, and failure of artificial and natural slopes. In order to develop methodologies for assessing vulnerability to these hazards and for making spatial and temporal predictions, and to develop technologies for improving the performance of geotechnical works in urban areas, we studied: (1) seismic performance of river embankments; (2) water infiltration behavior and creep movement of decomposed granite slopes; and (3) landslides triggered in residential areas in valley fills and hills by the 2004 Chuetsu earthquake.

Keywords: environment, geo-hazards, hazard mapping, urban area, hillslopes, mountains

1. Introduction

Urban areas developed in lowlands have been rapidly expanding into the surrounding hills and mountains. This expansion increases hazards associated with geological and geotechnical processes as well as exposure of residents. In particular, liquefaction during earthquakes causes potential risks to infrastructures in urban areas. Failure of artificial and natural slopes poses potential threats to residents and communities; such disasters were unfortunately realized during the 23 October 2004 Chuetsu Earthquake.

The objective of this study is to develop methodologies for assessing vulnerability to these hazards and making spatial and temporal prediction, as well as proposing techniques for improving the performance of geotechnical works in urban areas.

This paper summarizes the study results focusing on the following priority issues:

(1) Seismic performance of river embankments

Failure of river embankments during earthquakes poses potential hazards to urban areas due to flooding and inundation. The conventional analytical method for evaluating the seismic vulnerability is based on the pseudo-static limit equilibrium method and is not capable for evaluating the settlements. In this study, a method based on effective stress analysis for simulating the varying degree of settlements is studied through a series of centrifuge model tests and analyses.

(2) Prediction of shallow landslides

Rainstorms have been inducing widespread distributed landslides, but water infiltration behavior within weathered materials has not been well understood. In addition, even shallow landslides seem to be preceded by creep movement, but the creep movement has not been studied in detail. We focus on these issues to make spatial and temporal predictions of shallow landslides. We monitored water infiltration behavior within a decomposed granite slope, which is one of the typical rocks susceptible to landslides, as well as creep movement of the surface loosened layer.

(3) Valley fills and artificial slopes have been increasing related to the development of new residential areas conveniently located near large cities. Landslides in these valley fills and hills pose immediate threats to residents. We studied the site characteristics of the landslides triggered by the 2004 Chuetsu Earthquake in the suburb of Nagaoka and Ojiya cities, central Japan.

2. Seismic performance of river embankments

2.1 Introduction

River embankments in urban areas are often constructed on old river channels and other loosely deposited sandy layers. These embankments often suffered serious damage during earthquakes. Failure of river embankments during earthquakes poses potential hazards to urban areas due to flooding and

inundation. These hazards may be caused by Tsunami run-up through a river or those caused by heavy rains before or immediately after the earthquakes. These hazards are typically governed by the settlements of the embankments. However, the conventional analytical method for evaluating the seismic vulnerability is based on the pseudo-static limit equilibrium method and is not capable for evaluating the settlements.

Ozutsumi et al (2002) performed a series of effective stress analyses of liquefaction-induced deformation in river embankments using an effective stress model developed by one of the authors and his colleagues (Iai et al, 1992) and found that this analytical tool has the potential ability to simulate the liquefaction-induced residual deformation during earthquakes. In this study, the capability of this analytical tool for simulating the varying degree of settlements is studied through a series of centrifuge model tests and analyses.

2.2 Case history of damage to embankments

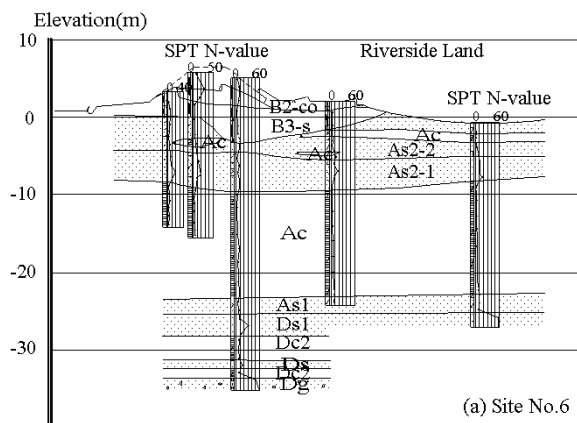
A case history of damage to the embankments at the mouth of the Yodo river in Osaka city, Japan, during 1995 Hyogoken Nambu earthquake (magnitude=7.2) was used as a reference in this study. This reference was systematically varied with respect to the level of shaking and foundation soil condition in the centrifuge model tests as described later.

The embankments were located within 40 km from the epicenter. The peak ground acceleration at the site of the embankments was about 0.2g as recorded at a nearby strong motion site (Matsuo et al, 2000). Typical damage to the embankments is shown in Fig. 1. The settlement of this embankment was 2.7 m. The other embankment located nearby settled only 0.3 m. These embankments were made of a core of soil materials covered with a concrete and asphalt as erosion protection and a parapet wall 8.1 m above the sea level.

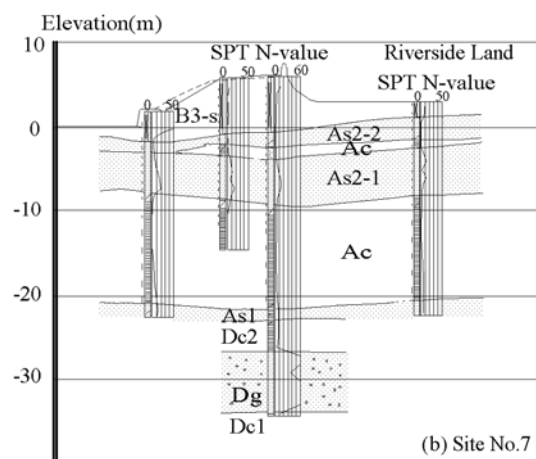
The cross sections and soil profiles of these embankments are shown in Fig.2 (JICE, 2002). These



Fig. 1 Typical damage to river embankments (Yodo river embankment during 1995 Hyogoken Nambu earthquake) (after Ozutsumi et al, 2002)



(a) Embankment with serious damage



(b) Embankment with minor damage

Fig. 2 Cross sections and soil profiles (after Ozutsumi et al, 2002)

embankments about 3 m high were constructed on a Holocene deposit about 20 m thick. The deposits consist of, from the top, the upper sandy layer (As2) about 10 m thick, clay layer (Ac) about 10 m thick and the lower sandy layer (As1) about 1 m thick. The SPT N-value of As2 layer is about 10. The soil profiles at both sites are similar to each other except for the existence of a cohesive layer Ac about 2 m thick below the embankment at the site of the embankment having smaller settlement as shown in Fig. 2(b). Foundation conditions significantly affect the seismic performance of embankments.

2.3 Centrifuge model tests of embankments

Centrifuge model tests were performed in 50g centrifugal acceleration using the geotechnical centrifuge at Disaster Prevention Research Institute, Kyoto University, with an arm length of 2.5 m. The cross section of an embankment was determined by referring to that at the Yodo river and shown in Fig. 3. The model embankment and foundation ground was made of Soma No.5 sand. The foundation ground condition was varied using a loose deposit for one series of tests, and a dense deposit for other. In each series of tests, amplitude of input motion was varied

in three levels. Total of six cases of mode tests were performed. Relative density of model foundation ground was about 30% for loose deposit, and 70% for dense deposit. Input motions were sinusoidal wave, 1Hz in prototype scale, with 20 cycles of loading.

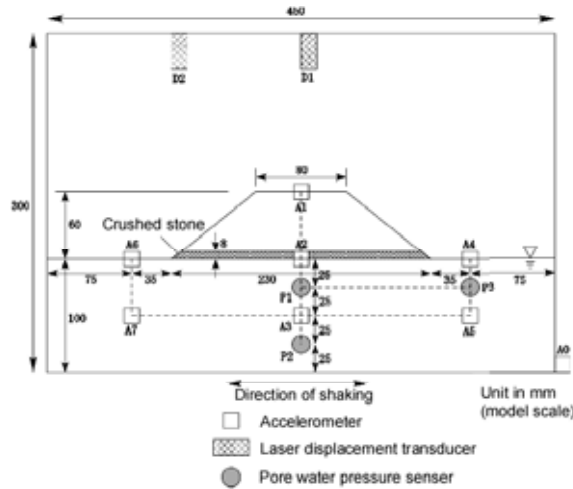


Fig. 3 Cross section of an embankment in centrifuge model tests (1/50 scaling at 50g field)

2.4 Results of centrifuge model tests

Typical examples of residual deformation of the embankment model are shown in Figs. 4 and 5. The one shown in Fig. 4 is the results for loose foundation ground subject to a peak acceleration of 313 Gal (Case3). Excess pore water pressures in the loose foundation ground gradually increased as cyclic shear is applied due to shaking. Foundation ground gradually softened due to the excess pore water pressure rise. The embankment pushed down the softened foundation ground, resulting in settlement at the crest associated with lateral spread deformation at the foundation ground.

The deformation shown in Fig. 5 is for dense foundation ground subject to a peak acceleration of 574 Gal (Case6). Failure mode of embankment in this case is represented by slide of embankment soil along the surface of embankment. Settlement of the crest is induced by this slide type of failure. There was no significant deformation in the dense foundation ground.

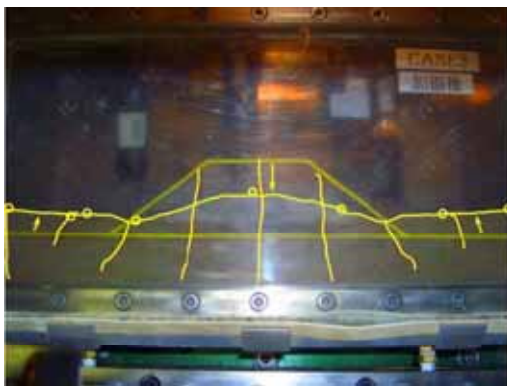


Fig. 4 Measured deformation of embankment on

loose foundation ground after shaking (Case3)

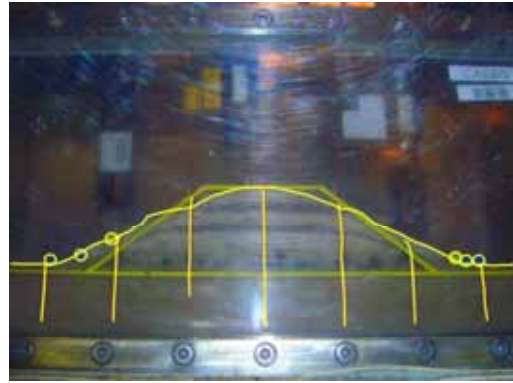


Fig. 5 Measured deformation of embankment on dense foundation ground after shaking (Case6)

2.5 Effective stress analysis through multiple shear mechanism model

The constitutive model used for the analysis is based on multiple inelastic shear mechanism model (Iai et al, 1992). The computer code incorporating this model is called FLIP (Finite element analysis of Liquefaction Program). The model takes into account the effect of rotation of principal stress axis directions, the effect of which is known to play an important role in the cyclic behavior of anisotropically consolidated sand. In addition to the conventional assumption of hyperbolic relationship assigned for each shear mechanism, the model uses the extended Masing rule to reproduce realistic hysteresis loop for cyclic loading. The excess pore water pressure generation due to dilatancy is modeled using the concept of liquefaction front, which is defined in the equivalent normalized stress space shown in Fig. 6, where S represents the mean stress ratio relative to the initial mean stress, and r represents the deviator stress ratio relative to the initial mean stress.

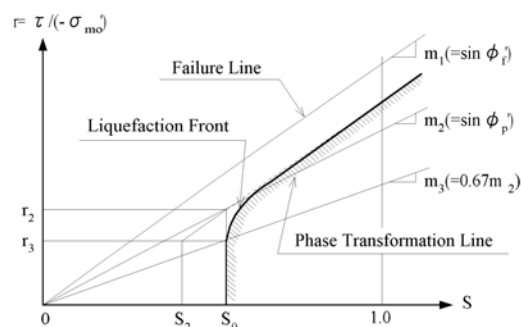


Fig. 6 Liquefaction front model

The analysis is performed in two steps. In the first step, static analysis is performed in drained condition by applying gravity (i.e. centrifugal acceleration in the model tests) over the analysis domain. In the second step, dynamic analysis is performed in undrained condition by applying input motion at the base of the analysis domain. The analysis in this study was performed for prototype scale with model

parameters that correspond to SPT N-value of 5 for loose foundation ground and 40 for dense foundation ground and the embankment.

Computed deformation of embankments is shown in Figs. 7 and 8. The one shown in Fig. 7 is the results for loose foundation ground.

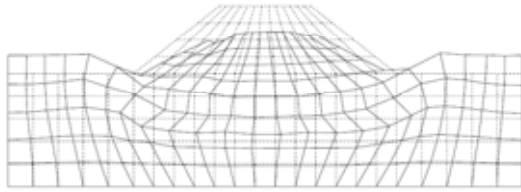


Fig. 7 Computed deformation of embankment on loose foundation ground after shaking (Case3)

mode is in good agreement with that measured and shown in Fig. 4. The agreements include the overall pattern of settlements associated with the lateral movement of foundation ground.

The computed deformation shown in Fig. 8 is for dense foundation ground. The agreement with the measured deformation shown in Fig. 5 is apparently not very good, especially the analysis was not successful in simulating the sliding of embankment slopes as shown in Fig. 5. This discrepancy is presumed to be due to the fact that, in the analysis, the nodes at both ends of the slopes share the same displacements as those of the foundation ground, whereas, in model tests, the soil of the embankment is free to slide over the foundation ground. If much finer meshes or other improvements in the analysis are adopted, the agreement would be improved. Within the scope of the present study, the results of analyses and model tests agreed in that deformation of embankment is confined within the embankment itself, without significant deformation in the dense foundation ground.

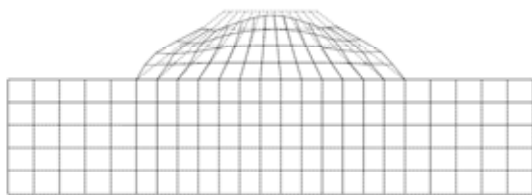


Fig. 8 Computed deformation of embankment on dense foundation ground after shaking

2.6 Settlement vs. acceleration level

In order to evaluate the overall performance of embankment subject to various levels of shaking, the measured and computed settlements obtained from all the six cases are shown in Fig. 9.

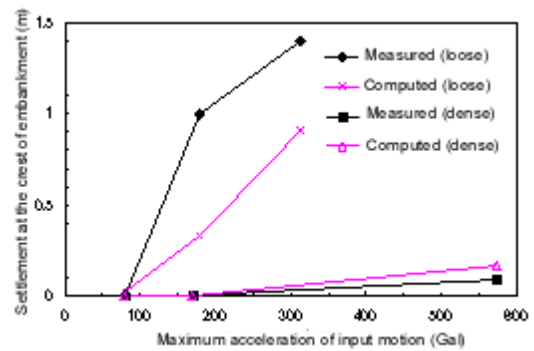


Fig. 9 Settlements at crest of embankment at various levels of acceleration

For a loose foundation ground, settlements reached 1.4 m at the maximum, equivalent to about 50% of the original height (3 m) of the embankment. For a dense foundation ground, the settlement was only 0.1 m at the maximum, equivalent to about 3% of the height of the embankment. Both the computed and measured results showed similar trends in settlements with increasing levels of shaking, although the computed results for loose foundation ground are smaller than those measured and the computed results for dense foundation ground are larger than those measured. In order to achieve better agreement, more studies may be necessary. The settlements for dense foundation ground are reduced to only 0.5 to 6.5% of those for loose foundation ground, indicating that the densification of foundation ground is effective in improving the performance of embankment.

2.7 Mechanism of settlement

In order to identify the mechanism of settlement in embankment, computed settlements are plotted in Fig. 10, superposed by the plot of axial strain difference in soil element in the foundation ground below the embankment. The results indicate that the settlement is closely correlated with the axial strain difference in foundation soil for loose condition. For dense foundation ground, the correlation is not good. Consequently, the settlement of embankment constructed on loose foundation ground is induced by deformation of foundation ground associated with axial strain difference of soil whereas the settlement of embankment on dense foundation ground is induced by due to deformation of embankment itself.

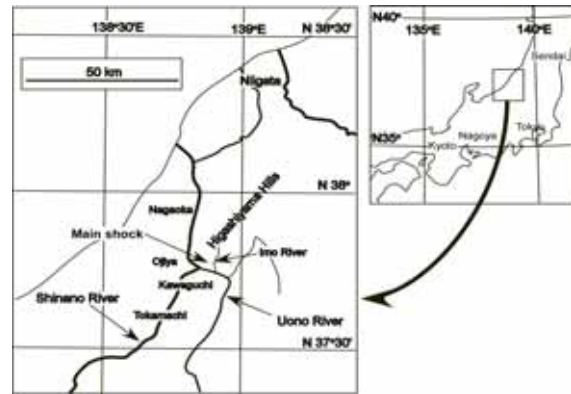
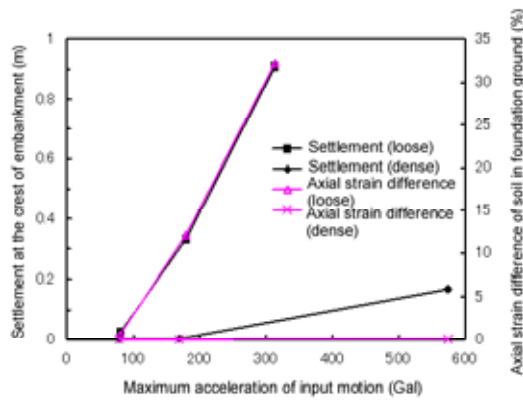


Fig. 10 Settlement and axial strain difference in foundation soil below the embankment

2.8 Summary

A series of centrifuge model tests and effective stress analyses were performed on performance of a river embankment during earthquakes. The following conclusions are obtained:

- (1) Settlements of embankments constructed on loose foundation ground are governed by deformation induced in the foundation ground, that settles and spread laterally.
- (2) Settlements of embankments constructed on dense foundation ground are governed by deformation in the embankment itself.
- (3) The effective stress analysis performed in this study captures the essential features of those seismic responses of embankment and can be a useful tool to assess the seismic performance of river embankment.
- (4) Condition of foundation ground significantly affects settlements of embankments. Densification of foundation ground is an effective measure to improve performance of embankments during earthquakes.

3. Landslides triggered by the 2004 Chuetsu earthquake

3.1 Outline of the earthquake

A series of earthquakes (the strongest with a magnitude of 6.8 in JMA-Japan Meteorological Agency; 6.5 on the Richter scale) and aftershocks jolted northern Japan on October 23, 2004, killing at least 30 people and injuring more than 2000 people largely as the result of building collapse. The strongest earthquakes with magnitudes greater than 6.0 on JMA scale occurred within a time frame of less than an hour, and had the epicenters spread across Ojiya city and Yamakoshi village, Niigata Prefecture. The major earthquakes were characterized by a shallow focal depth that generated strong levels of ground motion, resulting in extensive damage throughout the region. Hundreds of landslides were

triggered by the earthquakes and aftershocks with much associated to residential areas throughout southern Niigata Prefecture. Although heavy rain fell in the region two days prior to the earthquake, our field reconnaissance a few days after the earthquake revealed that most soils in shallower failures were relatively dry or only slightly wet along the sliding



surface.

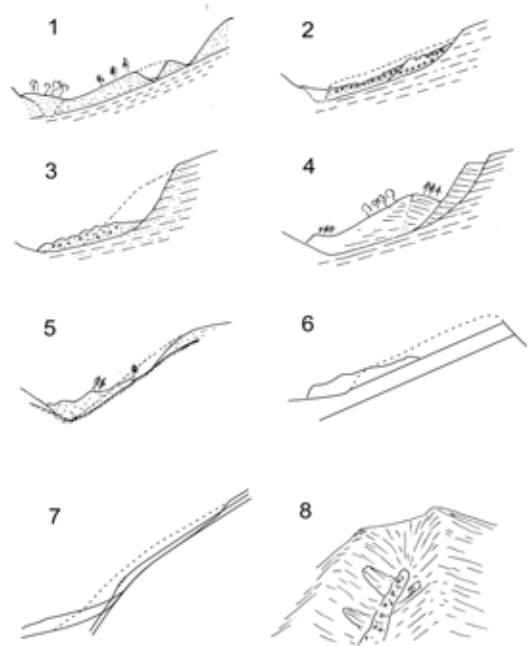
3.2 Landslides in roads and residential areas

Residential development, particularly cuts and artificial fills, is known to decrease slope stability (Sidle et al., 1985; Kamai et al., 2004). Earthquakes exacerbate such potential instabilities by the ground motion induced and the enhancement of pore water pressure in wet soils. Within our reconnaissance area, we observed earthquake triggered landslides that were highly affected by road cuts, road fills, and residential fills. Road cuts remove support along the uphill side of road corridors (Sidle et al., 1985; Megahan, 1986); thus, ground motion arising during an earthquake often triggers numerous landslides in these sites. Road fill materials on hillslopes naturally destabilize road embankments by adding weight to the hillslope, oversteepening the outside side of the embankment, and sometimes incorporating poor materials or insufficient consolidation of materials within the embankment. Hundreds of road cut slope and fillslope failures we observed as the result of the October 23rd earthquake. Additionally, much cut and fillslope material remained tenuously unstable awaiting failure during forthcoming rainstorms or periods of snowmelt.

Additionally, we investigated numerous failures triggered by the Chuetsu earthquake in residential fill slopes constructed on reclaimed land in Nagaoka city. Damages to houses and roads due to earthquake-induced landslides in Otoyoshi shuraku of Nagaoka city were significant (Fig. 12b,c). The entire housing development (Fig. 12a) was actually built on an old earthflow that was reactivated during the 23 October 2004 earthquakes. The tension crack in Fig. 12 b is evidence of the earthquake-induced reactivation of the earthflow, whereas the damaged house and road in Fig. 12 c is a consequence of the earthquake-induced failure of a valley fill. The geological structure in this area is Middle Pleistocene sediments, consisting of gravel, sand and mud (with weathered reddish soil) (Kobayashi et al., 1991).

Another residential area (Takamachi danchi) of Nagaoka city incurred substantial damage to houses and roads due to seismically-induced failures of artificial fill slopes. The entire road surrounding this development was constructed on fill material; the road was partly destroyed during the earthquake. Takamachi danchi covers about 4.1 ha, and lies on Pliocene to Middle Pleistocene sediments composed of sand, silt and gravel. About 70 of the 522 homes in the development were damaged due to seismically-induced deformations and failures of artificial fill slopes. Apparently, the fill material in both Otoyoshi and Takamachi regions was partly saturated partly due to the rainstorms during the previous series of typhoons that struck the region a few days prior to the earthquake. Poor drainage systems within the retaining structures supporting the fill contributed to the accumulation of water in the fill

slopes and exacerbated the instability.



3.3 Geological and geomorphological characteristics of landslides

Thousands of landslides of natural slopes occurred in hilly areas in the Higashiyama Hills, where Plio-Pleistocene sedimentary rocks are distributed. The most common landslides of natural slopes triggered by the earthquake were shallow disrupted landslides on steep slopes without geologic



preference, which has been common to many previous disastrous earthquakes in the world (KEEFER, 1984). The Chuetsu earthquake also triggered many deep landslides, damming streams and flooding villages. Field investigation and interpretation of aerial photographs taken before and after the earthquake clarified that many of these slides had occurred due to the reactivation of previous landslides (CHIGIRA, 2004). These had planar sliding surfaces along bedding planes or along the oxidation front (Fig. 13). The bedding-parallel sliding surfaces were made at the boundary between the overlying permeable sandstone and underlying siltstone (1 in Fig. 13, Fig. 14) or along the bedding planes of the alternated beds of sandstone and siltstone (2, 3, and 4 in Fig. 13). Sliding surfaces along the oxidation front were made in the area of marine black mudstone (5 in Fig. 13). New landslides (rockslide-avalanches) occurred with the sliding surfaces in an a-few-cm thick tuff interbedded in siltstone (6 in Fig. 13). Most of the deep landslides occurred on slopes undercut by erosion or artificial excavation, notwithstanding they were reactivated or new ones. One rockslide-avalanche occurred on a slope where buckling deformation preceded the earthquake (7 in Fig. 13). Gentle valley bottom sediments were mobilized in many locations, probably because they were saturated and partial liquefaction occurred by the earthquake (8 in Fig. 13).

3.4 Summary

The 2004 Chuetsu earthquake triggered many landslides of road cut slopes, residential fill slopes in urban area, as well as on natural slopes, isolating villages. Precipitation of about 100 mm two days before the earthquake seems to have affected the landslide. The most common landslides of natural slopes were shallow disrupting landslides, but more than 100 deep slides also occurred and affected wide areas and dammed streams. Most of these deep slides were due to the reactivation of old landslides and had planar sliding surfaces along bedding planes or the oxidation front. In addition, most of the deep slides were undercut before the earthquake and destabilized. Mobilization of sediments filling gentle valleys also occurred.

4. Stability of urban natural slopes

Urban areas are growing into neighboring mountainous areas by cutting natural slopes or by utilizing areas at the foot of mountain slopes. Particularly, Japan has very small flat areas, so this situation is becoming very common.

4.1 Water filtration behavior within decomposed granite

One of the rock types, which are very susceptible to landslides and has been suffering serious damage by rainstorms, is granite (Fig. 15, (CHIGIRA, 2001).

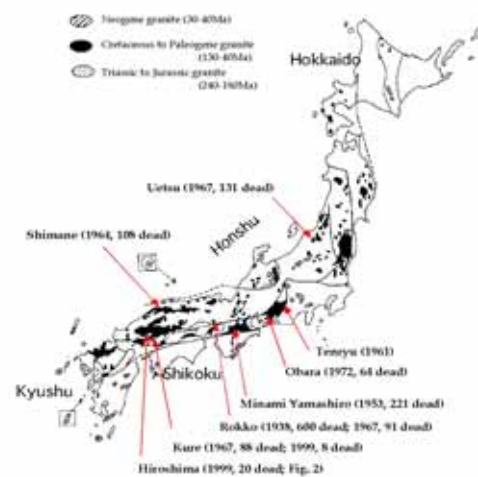


Fig. 15 Landslide disasters occurred in the granitic rock areas.

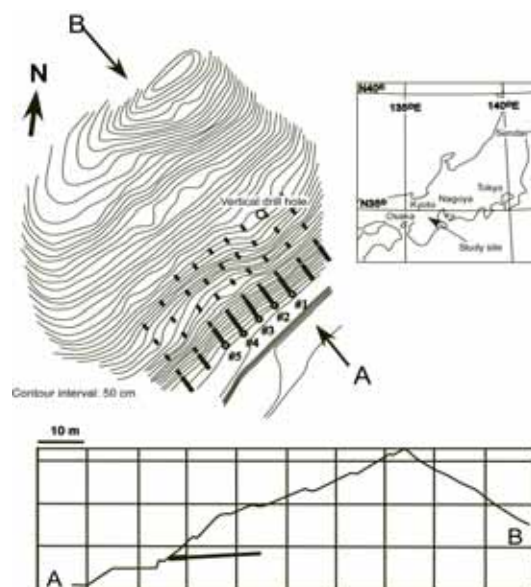


Fig. 16 Locality and topographic map and a cross section of the study site.

Granite occupies wide areas in urban areas and also in candidate sites of new Japanese capital, partly because it forms wide low-relief hills and are easily excavated by machine without explosion. In spite of the above situation, landslide mechanism of weathered granite is not well understood so spatial and time prediction methodology of those landslides is not yet developed.

In order to clarify the mechanism of landslide of weathered granite and water filtration behavior, which is essential to establish the methodology to predict landslide by rainstorms, we monitored water filtration behavior and surface creep movement of a decomposed granite slope. Details of the results and the conceptual model of water filtration have been

written in a paper submitted elsewhere (CHIGIRA et al., submitted).

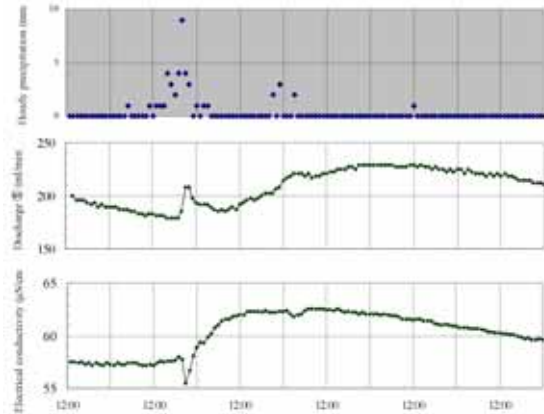
(1) Study site and methods

The investigation site is located in the southern part of Shiga Prefecture, central Japan (Fig. 16). This site is a hilly area with elevations from 450 to 650 m above sea level, and is underlain by the Cretaceous Shigaraki granite (Collaborative Research Group for the Granites around Lake Biwa, 1982). The landform has low relief with a relative height of less than one hundred meters from flat river bottom. The granite is deeply weathered, and almost all outcrops above the river bottom consist of decomposed granite except for sporadically exposed core stones, while beneath the stream bottom less weathered and sound granite rock is expected. This area was struck by a heavy rainstorm in 1953; widely distributed, destructive landslides occurred, killing forty-four people.

We monitored rainfall, discharge amount, electrical conductivity and the chemistry of water from sub-horizontal drill holes just beneath the groundwater table within a decomposed granite slope as well as suction and creep movement at the slope surface (Fig.16). The monitoring interval was from April 2003 to November 2004. Water sampling for chemical analysis was done manually.

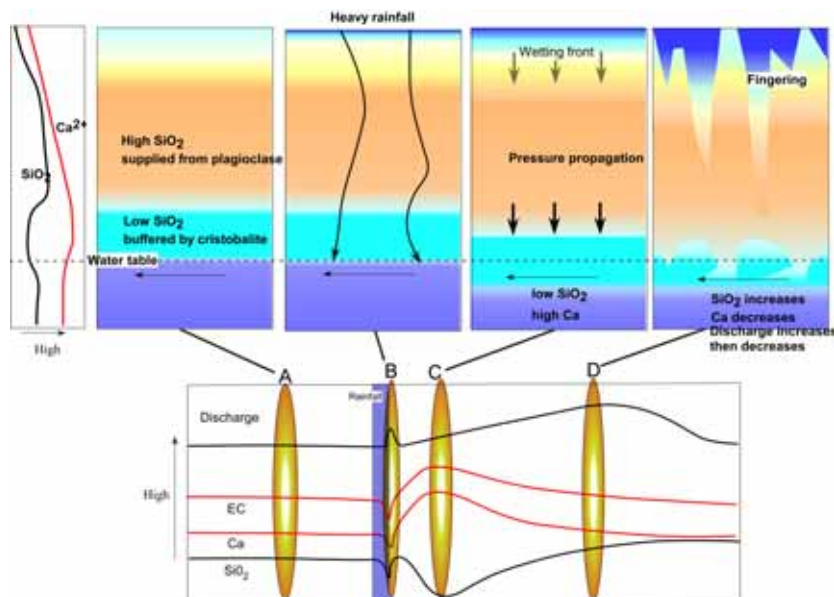
(2) Results and a conceptual model of water filtration

Typical response of electrical conductivity and discharge amount against rainfall events is shown in Fig. 17. We found that when precipitation exceeds about 30 mm, electrical conductivity decreases spontaneously, then soil water with high electrical conductivity is pushed down and subsequently dilute rainwater itself reaches to the groundwater table. The conceptual model of water filtration suggested by the monitoring results is shown in Fig. 18. The pushing down occurs at almost all rainfall events exceeding 10 mm precipitation. The immediate decrease of the electrical conductivity is due to quick inflow of rainwater to the groundwater table through “express ways” like cracks, and its increase is due to the



pushing down of soil water. The electrical conductivity reached to its maximum 20 to 40 hours after the peak of rainfall events and then decreased, while the discharge from the drill holes increased further after the peak of the electrical conductivity to become its maximum 2 to 5 days after the peaks of precipitation. The time delay of the maximum of discharge amount from the maximum of the electric conductivity suggests that the pushing down of the soil water is caused by the pressure propagation by the downward movement of the wetting front as was suggested by Bianchi and Haskell (1966).

The soil water that is pushed down seems to be a capillary water above the groundwater table. The SiO₂ concentration of this water is apparently controlled by the solubility of cristobalite and is rich in Ca, which is supplied from plagioclase with SiO₂. The cation concentrations in the unsaturated soil water and the capillary water are affected by ion exchange.



4.2 Creep movement of a surface loosened layer

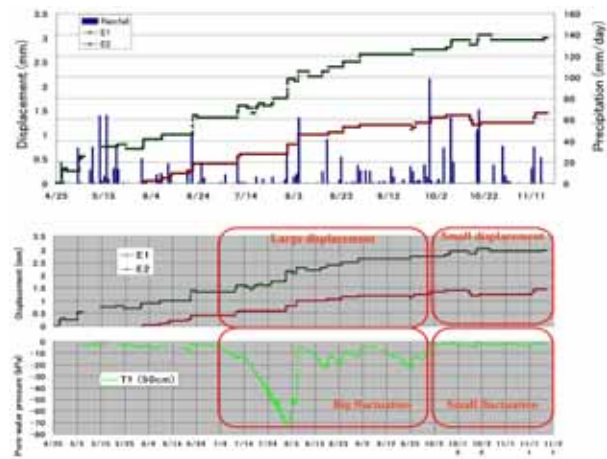
Surface deformation by creep movement of a loosened layer was observed on the monitored slope. Figure 19 shows the displacements measured with extensometers along with precipitation and matric suctions in the loosened layer in the depth of 50 cm. Monitored suction data indicated that positive pore water pressure occurred only several times during the monitored interval. Accumulated creep displacement during 7 months was about 3 mm. The displacement was not directly related to the amount of precipitation but to the fluctuation ranges of matric suction as is seen in Fig. 19. In July and August, there were not so heavy rainstorms in comparison with the other months, but most of the displacement occurred. Figure 19 also shows that the fluctuation ranges of suction were the largest in these two months. These findings indicate that displacement occurs in response to the repetition of wetting and drying rather than to positive pore pressures.

4.3 Summary

Water infiltration behavior observed by the monitoring the amount, chemistry, and electrical conductivity of water from just beneath the groundwater table in decomposed granite suggests that infiltration near the groundwater table has three steps: Quick inflow through short-cuts like cracks, pushing down of the capillary water, and then inflow of rainwater through matrix of decomposed granite. The surface loosened layer creeps in response to the repetition of drying and wetting before catastrophic sliding.

5. Concluding remarks

During this fiscal year, we performed the studies on (1) seismic performance of river embankments, (2) water infiltration behavior and creep movement of decomposed granite slope, and (3) landslides triggered in residential areas in roads, valley fills and hills by the 2004 Chuetsu earthquake. In addition to the study in FY 2003, which includes (1) performance of retaining walls at waste fill in waterfront areas, (2) hazard mapping of natural slope failures through monitoring using laser scanners, and (3) hazard assessment of residential areas in valley fills, we are approaching to our goal, to develop methodologies for assessing vulnerability to geohazards and for making spatial and temporal prediction, and to propose techniques for improving the performance of



geotechnical works in urban areas.

Acknowledgements

The authors are grateful to former students, Chizuru Imai and Hideaki Hijikata for performing geohydrological monitoring in the field.

References

- Bianchi, W. C. and Haskell, E. E. J. (1966): Air in the vadose zone as it affects water movements beneath. *Water Resources Research*, Vol. 2, pp.315-322.
- Chigira, M. (2001): Micro-sheeting of granite and its relationship with landsliding specifically after the heavy rainstorm in June 1999, Hiroshima Prefecture, Japan. *Engineering Geology*, Vol.59, pp.219-231.
- Chigira, M. (2004): Geological and geomorphological characteristics of landslides generated by the Chuetsu Earthquake. Report of the 2004 Chuetsu Earthquake Disaster, Japan Landslide Society and the Japan Society of Engineering Geology, pp.12-21. (In Japanese)
- Chigira, M., Imai, C., and Hijikata, H. (submitted): Water percolating behavior indicated by the water chemistry within a decomposed granite slope, central Japan. Submitted to *Engineering Geology*.
- Collaborative Research Group for the Granites around Lake Biwa (1982): Granitic masses around Lake Biwa, Southwest Japan - on the granites in the Koga area -. *Journal of the Geological Society of Japan*, Vol. 88, pp.289-298.
- Iai, S., Matsunaga, Y. and Kameoka, T. (1992): Strain

- space plasticity model for cyclic mobility, *Soils and Foundations*, Vol.32, No.2, pp.1-15.
- Japan Institute of Construction Engineering (JICE) (2002): Numerical analysis methods of evaluating earthquake-induced deformation in river dikes, JICE2001 (in Japanese)
- Kamai, T., Shuzui, H., Kasahara, R., and Kobayashi, Y. (2004): Earthquake risk assessments of large residential fill-slope in urban areas. *Journal of the Japan Landslide Society*, Vol. 40, pp.389-399.
- Keefer, D. (1984): Landslides caused by earthquakes. *Geological Society of America Bulletin*, Vol. 95, pp.406-421.
- Kobayashi, I., Tateishi, M., Yoshioka, T., and Shimazu, M. (1991): Geology of the Nagaoka district, with geological sheet map at 1:50,000, Geological Survey of Japan, 132 pp. (in Japanese with English abstract)
- Matsuo, O., Okamura, M. Uzuoka, R. and Mihara, M. (2000): Numerical analyses of the damaged dikes in the 1995 Hyogo-ken Nanbu earthquake, Proc. 12th World Conference on Earthquake Engineering, CD-ROM.
- Megahan, W.F. (1986): Roads and forest site productivity. In: *Degradation of forest land: "forest soils at risk"* (J.D. Lousier & D.W. Stills, eds.), Land Management Report, No. 56, Ministry of Forestry, USA, pp. 54-65.
- Ozutsumi, O., Sawada, S., Iai, S., Takeshima, Y., Sugiyama, W., and Shimazu, T. (2002): Effective stress analyses of liquefaction-induced deformation in river dikes, *Soil Dynamics and Earthquake Engineering*, Vol.22, pp.1075-1082.
- Sidle, R.C., A.J. Pearce, and C.L. O'Loughlin (1985): *Hillslope stability and land use*, Water Resources Monograph, Vol. 11, American Geophysical Union, Washington, DC, 140 pp.

都市および周辺地域における地盤災害予測とハザードマッピングに関する研究
平成16年度報告

千木良雅弘, 井合 進, Sidle R.C., 釜井俊孝,
三村 衛, 諏訪 浩, 斉藤隆志, 飛田哲男

要旨

本研究は、地震時液状化、宅地造成地盤崩壊、人工・自然斜面崩壊などの地盤災害に対する都市域の脆弱性診断技術と危険度評価技術の高度化、発生場の時空的予測技術の開発、地盤基礎構造物の性能向上技術の開発を目的とする。平成16年度のとりまとめとして、本論文では、河川堤防の耐震性能、風化花崗岩斜面内の地下水浸透挙動、表層土のクリープ挙動、2004年中越地震によって発生した斜面移動現象の発生場についてとりまとめた。

キーワード: 環境, 危険度評価, 丘陵地, 山地, 地盤災害

都市および周辺地域における地盤災害予測とハザードマッピングに関する研究
平成16年度報告

千木良雅弘，井合 進，Sidle R.C.，釜井俊孝
三村 衛，諏訪 浩，斉藤隆志，飛田哲男

1. はじめに

低平地を中心として急速に周辺丘陵地へと拡大する都市域では、地震時液状化、宅地造成地盤崩壊、人工・自然斜面崩壊など、地盤災害の危険性が増している。本研究は、これらの地盤災害に対する都市域の脆弱性診断技術と危険度評価技術の高度化、発生の時と場所の予測技術の高度化、地盤基礎構造物の性能向上技術の開発を目的とする。平成16年度のとりまとめとして、本論文では、河川堤防の耐震性能向上、2004年中越地震によって発生した地すべり・斜面崩壊現象の発生場の解明、風化花崗岩斜面内の降雨浸透挙動に関する研究結果をとりまとめた。

2. 河川堤防の耐震性能

低平地に展開する都市域の耐水土構造物の耐震性能の診断技術の高度化を目的として、河川堤防を対象として、遠心力場の模型振動実験および有効応力解析を行った。既往の耐震性診断技術としては、等価静的慣性力などを考慮した力のバランスに基づく簡易解析法（円弧すべり法）があるが、この方法では、耐震性能を支配する堤防天端の沈下量を予測することができない。対象とした断面は、1995年兵庫県南部地震において液状化により崩壊した淀川堤防（高さ3m）である。遠心力場の実験では、基礎地盤（飽和砂地盤）の条件を緩詰めおよび密詰めの場合の2種類の条件、それぞれの地盤条件において入力波の振幅を変化させて3ケースずつ、延べ6ケース実施した。基礎地盤が緩詰めの場合には、基礎地盤を堤防が押し下げる形で堤防の沈下が発生したのに対し、基礎地盤が密詰めの場合には、堤防盛土部分の表層すべりによる沈下となっている。これらの堤防の変形形態は、有効応力解析により、概ね再現できることが確認された。また、沈下量についても、概略レベルではあるが、有効応力解析により再現可能であることが確認された。あわせて、河川堤防の耐震性能向上のためには、地盤の締固めなどによる基礎地盤の耐震性向上が著しい効果を発揮することが明らかにされた。

3. 2004年中越地震による斜面変動現象

2004年中越地震は、代表的な地すべり地帯で、

しかも長岡市や小千谷市といった都市とその近郊山地の直下を震源として発生した。その結果、1000を超える膨大な数の地すべりと崩壊が発生し、丘陵に拡大していった住宅地の地盤に変形を生じ、また、山間地の集落を孤立させた。2004年中越地震は、いわばわが国の地方都市に発生する地震災害の典型的な事例でもあった。

長岡市の丘陵を造成した住宅地では、いたるところで盛り土がすべった。特に、不安定になった盛り土下の旧谷の方向と地震動の方向との間に関連が見られた。より山地側では、地すべりと表装崩壊が数多く発生し、川が閉塞され、一部の集落は水没した。比較的規模の大きかった地すべりの大部分は古い地すべりの再活動であり、また、それらは脚部を侵食などによって切り取られており、不安定化していたものであった。これらの結果は地震時に発生する地すべり危険箇所の判定に大きな参考となる。

4. 風化花崗岩斜面内の降雨浸透挙動と表層クリープ

花崗岩はわが国の主要都市の近郊に広く分布し、都市は、その分布域に拡大している。また、花崗岩は首都機能移転候補地にも広く分布している。一方で、風化花崗岩は従来の豪雨によって数多く崩壊してきたが、その崩壊メカニズムについては不明な点が多く残されている。そこで、風化花崗岩斜面において、表層のサクシオンと地下水面近傍からの水の量、化学組成、電気伝導度を連続的に観測した。その結果、強い降雨があると、降水は最初短絡経路を通過して地下水面に達し、その後風化花崗岩を浸透する水が毛管帯の水を押し下げ、その後降水そのものが地下水面に到達する、といった現象が連続的に起こることがわかった。実際の崩壊は地下水面が上昇、あるいは表層の緩み帯に宙水が形成して発生するものと考えられるが、その前段階の浸透挙動が明らかになったといえる。

風化花崗岩の表層での変位測定結果では、表層の変位は、特に強い降雨の時に大きく発生するというよりも、サクシオンが大きく変動する期間に特に集中することが明らかになった。これは、崩壊の発生に至るような注意すべき降雨パターンに示唆を与える。